



A new $\text{Ca}_3\text{MgSi}_2\text{O}_8$ compound and some of its thermodynamic properties



Xinjian Bao^{a,b}, Yanyao Zhang^{a,b}, Zhigang Zhang^c, Lifei Zhang^{a,b}, Xiaoyang Liu^d, Jianjun Dong^e, Xi Liu^{a,b,*}

^a Key Laboratory of Orogenic Belts and Crustal Evolution, MOE, Peking University, Beijing 100871, China

^b School of Earth and Space Sciences, Peking University, Beijing 100871, China

^c Key Laboratory of Earth and Planetary Physics, Institute of Geology and Geophysics, Chinese Academy of Sciences, Beijing 100029, China

^d State Key Laboratory of Inorganic Synthesis and Preparative Chemistry, College of Chemistry, Jilin University, Changchun 130012, China

^e Physics Department, Auburn University, Auburn, AL 36830, USA

ARTICLE INFO

Keywords:

New $\text{Ca}_3\text{MgSi}_2\text{O}_8$ compound
Single-crystal X-ray diffraction
First-principles simulation
Compressibility
Heat capacity
Standard vibrational entropy

ABSTRACT

A new calcium magnesium orthosilicate with the composition $\text{Ca}_3\text{MgSi}_2\text{O}_8$ was synthesized by a solid-state reaction process at 1.2 GPa and 1373 K for 7 days. We refined the crystallographic structure of this new compound using single-crystal X-ray data, and obtained some of its thermodynamic properties by performing some first-principles simulations. Our single-crystal X-ray analysis has shown that this new compound is monoclinic with the space group $C2/c$, and its unit-cell parameters are $a = 9.344(4) \text{ \AA}$, $b = 5.3308(3) \text{ \AA}$, $c = 13.290(6) \text{ \AA}$, $\alpha = 90^\circ$, $\beta = 92.072(7)^\circ$, $\gamma = 90^\circ$, and $V = 658.7(6) \text{ \AA}^3$. The compressibility of this new compound was studied with the CASTEP code using density functional theory and planewave pseudopotential technique, which led to an isothermal bulk modulus B_0 of 99(2) GPa with a pressure derivative B_0' of 3.5(5). The phonon dispersions and vibrational density of the states (VDoS) of this new compound were calculated by using density functional perturbation theory. Subsequently, the VDoS was combined with a quasi-harmonic approximation to compute the isobaric heat capacity (C_p) and standard vibrational entropy (S_{298}^0), yielding $C_p = 3.927(2) \times 10^2 - 1.159(6) \times 10^3 T^{-0.5} - 1.054(4) \times 10^7 T^{-2} + 1.362(8) \times 10^9 T^{-3} \text{ J mol}^{-1} \text{ K}^{-1}$ for the T range of 298–1000 K and $S_{298}^0 = 270.5(60) \text{ J mol}^{-1} \text{ K}^{-1}$.

1. Introduction

The calcium magnesium orthosilicates have attracted much attention for their wide applications as cements, photoluminescent materials and bioactive materials due to their versatile structures as well as interesting physical and chemical properties [1–3]. These compounds are also found as mineral inclusions in diamonds originated from the Earth's mantle [4], and may be used to estimate the formation P-T conditions of the diamonds [5].

The composition $\text{Ca}_3\text{MgSi}_2\text{O}_8$ was previously demonstrated to crystallize into the phase merwinite (space group $P21/a$, $Z = 4$), one of the calcium magnesium orthosilicates. Since the structure of merwinite is much more closely-packed than that of olivine, merwinite has been proposed as a possible stable phase in the upper mantle of the Earth [6]. Indeed, Liu experimentally demonstrated that merwinite was stable at 1273 K and 20 GPa [7]. In the lower mantle of the Earth, the perovskite-structured compounds MgSiO_3 and CaSiO_3 were thought to be the predominant phase. It has been shown that the crystal structure of merwinite consists of a perovskite-like layer of $[\text{MgO}_6]$ octahedra and a double-layer of $[\text{SiO}_4]$ tetrahedra, stacking

alternatively in the [111] direction of an ideal cubic perovskite structure [8]. The close relationship between the structure of merwinite and those of the MgSiO_3 and CaSiO_3 perovskites is very meaningful: Since the MgSiO_3 and CaSiO_3 perovskites are usually unquenchable, a good understanding about the structure and properties of merwinite may lead to better understanding of the structures and physical-chemical properties of the MgSiO_3 and CaSiO_3 perovskites.

In this work, we synthesized a new compound, with the composition $\text{Ca}_3\text{MgSi}_2\text{O}_8$ but a structure slightly different to that of merwinite, using a solid-state reaction method. The crystallographic details of this new phase were obtained by performing single-crystal X-ray diffraction analysis. First-principles calculation was engaged to study some of the thermodynamic properties of this new phase. With the CASTEP code, the compressibility was determined by using density functional theory and planewave pseudopotential technique, and the phonon dispersions and vibrational density of the states (VDoS) were calculated by using density functional perturbation theory. The VDoS was further combined with a quasi-harmonic approximation to compute the isobaric heat capacity (C_p) and standard vibrational entropy (S_{298}^0).

* Corresponding author at: Key Laboratory of Orogenic Belts and Crustal Evolution, MOE, Peking University, Beijing 100871, China.
E-mail address: xi.liu@pku.edu.cn (X. Liu).

2. Experimental and theoretical section

2.1. Synthesis

A new calcium magnesium orthosilicate with the composition $\text{Ca}_3\text{MgSi}_2\text{O}_8$ was synthesized by a solid-state reaction method. The starting material was made as following: (1) pure chemicals CaCO_3 (Alfa Aesar, powder, 99.9%), MgO (Alfa Aesar, powder, 99.9%) and SiO_2 (Alfa Aesar, powder, 99.9%) were pretreated at 1 atm and 723 K for 72 h, mixed in a mole ratio 3:1:2, and ground and homogenized in a agate mortar; (2) this mixture was pressed into a pellet and degassed in a Pt crucible at 1 atm and 1273 K for 48 h; (3) the degassed pellet was crushed into a fine powder, which was further stored in a drying oven at 383 K for later synthesizing experiment. The starting material was loaded into a Pt capsule (10 mm in length and 2.5 mm in diameter), which was sealed at both ends using an arc-welding technique. Our synthesizing experiment was carried out with a piston-cylinder apparatus installed in the High-Pressure Laboratory of Peking University (Depths of The Earth Company Quickpres [9,10]). The experimental assembly and high- P experimental technique were generally identical to those reported in [11]. Our sample was synthesized at 1.2 GPa and 1373 K with a heating time of 7 days.

2.2. Characterization

The synthetic product was polished with a series of diamond pastes, washed with an ultrasonic washing machine, carbon-coated and examined with an electron microprobe (EMP; JEOL JXA-8100). The analyses were carried out in twenty-two randomly-selected areas. The sample was then slowly ground down to a fine powder and checked with a powder X-ray diffractometer (Rigaku D/Max 2550V/PC with graphite-monochromated Cu K α radiation) at ambient conditions.

2.3. Single-crystal X-ray diffraction

Suitable single crystal of the new $\text{Ca}_3\text{MgSi}_2\text{O}_8$ compound was selected for single-crystal X-ray diffraction analysis. Intensity data was collected on a Bruker Smart ApexII Quazar micro-focused diffractometer using Mo K α radiation ($\lambda = 0.71073$ nm). The raw data was processed and corrected for the absorption effects using SAINT+ and SADAB. An initial structure solution was obtained via direct methods and refined by a full-matrix least-squares method using the SHELXT software included in the SHELXTL package. All heaviest atoms were first located unambiguously in the Fourier maps, and then the O atoms were found in the subsequent difference maps. All atoms were refined with anisotropic displacement parameters. The final cycles of the least-squares refinement including atomic coordinates and anisotropic thermal parameters for the atoms [$I > 2\sigma(I)$] converged at $R_1 = 0.0527$, $wR_2 = 0.1310$, and $S = 1.035$ for this new $\text{Ca}_3\text{MgSi}_2\text{O}_8$ compound.

2.4. Computational method

The first-principles simulation carried out to investigate the compressibility of the new $\text{Ca}_3\text{MgSi}_2\text{O}_8$ compound was completed with the CASTEP code using density functional theory [12,13] and planewave pseudopotential technique [14]. The exchange-correlation interaction was treated by the generalized gradient approximation (GGA) with the Perdew-Burker-Ernzerhof (PBE) functional [15], and a convergence criterion of 10^{-6} eV/atom was used in the self-consistent field calculations. We employed a planewave basis set with a cutoff of 990 eV to expand the electronic wave functions, and a norm-conserving pseudopotential to model the ion-electron interaction [16,17]. We sampled the irreducible Brillouin zone with a $3 \times 3 \times 1$ Monkhorst-Pack grid [18]. The effects of using larger cutoff and k point mesh on the calculated properties were found to be insignificant. The computation cell

contained four $\text{Ca}_3\text{MgSi}_2\text{O}_8$ molecules (in total 56 atoms), with the initial structure model from our single-crystal X-ray analysis. The equilibrium lattice parameters and internal coordinates at different pressures were optimized by minimizing the Hellmann-Feynman force on the atoms and simultaneously matching the stress on the unit cell to the target stress. These theoretical techniques were used in our previous studies targeting the structures and thermodynamics of some silicate minerals [19,20].

Based on the optimized structure with the GGA + PBE method, the phonon dispersions and VDoS of the $\text{Ca}_3\text{MgSi}_2\text{O}_8$ compound were calculated by diagonalizing the dynamical matrix whose elements were obtained using density functional perturbation theory [21,22]. The q-vector grid spacing for interpolation was 0.07 \AA^{-1} , which represented the average distance between the Monkhorst-Pack q-points used in the dynamical matrix calculations. The phonon dispersions were obtained at the high symmetry points (L, M, A, G, Z, V). The coordinates of these points on the surface of the Brillouin zone were $L = (-1/2, 0, 1/2)$, $M = (-1/2, -1/2, 1/2)$, $A = (-1/2, 0, 0)$, $G = (0, 0, 0)$, $Z = (0, -1/2, 1/2)$, $V = (0, 0, 1/2)$.

3. Results and discussion

3.1. Phases in synthetic material

The electron back-scatter images (Fig. S1) indicate that there is just one crystalline phase appearing in our synthetic product, but the powder X-ray diffraction data (Fig. 1) show that another crystalline phase with a small proportion occurs. This minor phase could be a pyroxene, as implied by the powder X-ray diffraction data. The 22 EMP analyses suggest a chemical formula of $\text{Ca}_{3.04(2)}\text{Mg}_{1.00(1)}\text{Si}_{1.98(1)}\text{O}_8$ for the major phase, close to an idealized formula of $\text{Ca}_3\text{MgSi}_2\text{O}_8$.

3.2. Single-crystal structure

The single-crystal analysis of the new $\text{Ca}_3\text{MgSi}_2\text{O}_8$ compound reveals that it crystallizes in the $C2/c$ space group, rather than in the $P21/a$ space group of the merwinite, with $a = 9.344(4) \text{ \AA}$, $b = 5.308(3) \text{ \AA}$, $c = 13.290(6) \text{ \AA}$, $\alpha = 90^\circ$, $\beta = 92.072(7)^\circ$, $\gamma = 90^\circ$, and $V = 658.7(6) \text{ \AA}^3$ (Table 1), in agreement with those obtained by our powder X-ray diffraction pattern (Fig. 1).

Each asymmetric unit contains one distinct Mg site, one distinct Si site, two distinct Ca sites and four distinct O sites (Fig. S2), and their coordinates and equivalent isotropic displacement parameters are listed in Table S1. As shown in Fig. 2 and Table S2, the Mg atom is

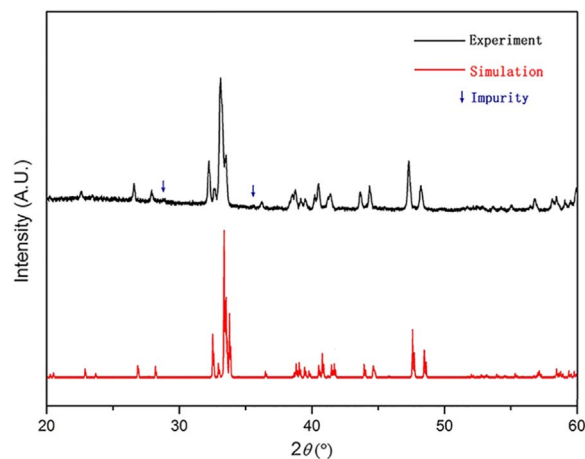


Fig. 1. Experimental and simulated powder X-ray diffraction patterns of the new $\text{Ca}_3\text{MgSi}_2\text{O}_8$ compound. The simulated pattern is based on the structure refined by our single-crystal X-ray diffraction analysis. The arrows indicate those extremely weak peaks in the experimental powder X-ray diffraction pattern, which do not belong to the new $\text{Ca}_3\text{MgSi}_2\text{O}_8$ compound.

Table 1
Crystal data and structure refinement for the new $\text{Ca}_3\text{MgSi}_2\text{O}_8$ compound.

| Empirical formula | $\text{Ca}_3\text{MgSi}_2\text{O}_8$ |
|---------------------------------|---|
| Formula weight | 328.73 |
| Temperature | 293(2) K |
| Wavelength | 0.71073 Å |
| Crystal system, space group | Monoclinic, $C2/c$ |
| Unit cell dimensions | $a = 9.344(4)$ Å $b = 5.308(3)$ Å $c = 13.290(6)$ Å $\alpha = 90^\circ$ $\beta = 92.07(7)^\circ$ $\gamma = 90^\circ$ |
| Volume | $658.7(6)$ Å ³ |
| Z | 4 |
| Crystal size | $0.1 \times 0.08 \times 0.08$ mm |
| Theta range for data collection | $3.07\text{--}26.32^\circ$ |
| Limiting indices | $-10 \leq h \leq 11, -4 \leq k \leq 6, -14 \leq l \leq 16$ |
| Reflections collected/unique | 1762/671 [R(int) = 0.0629] |
| Completeness to theta = 25.10 | 99.60% |
| Refinement method | Full-matrix least-squares on F^2 |
| Data/restraints/parameters | 671/0/66 |
| Goodness-of-fit on F^2 | 1.035 |
| Final R indices [I > 2sigma(I)] | $R_1 = 0.0527, wR_2 = 0.1310$ |
| R indices (all data) | $R_1 = 0.0709, wR_2 = 0.1412$ |
| Largest diff. peak and hole | 1.187 and $-1.014 e \text{ Å}^{-3}$ |

coordinated to six bridging O atoms to form a $[\text{MgO}_6]$ octahedron. The Mg-O bond lengths are in the range from 2.027(4) Å to 2.140(4) Å, while the O-Mg-O angles from 86.94(17)° to 180.0(2)°. All the Si atoms are in the 4-fold coordination to form $[\text{SiO}_4]$ tetrahedra. The Si-O bond lengths vary from 1.587(4) Å to 1.634(4) Å whereas the O-Si-O angles from 103.9(2)° to 117.3(2)°. The Ca(1) and Ca(2) are 8- and 6-coordinated, respectively, and the Ca(1)-O and Ca(2)-O bond lengths are in the range of 2.246(5)–2.778(5) Å and 2.307(5)–2.709(5) Å, respectively.

The new $\text{Ca}_3\text{MgSi}_2\text{O}_8$ compound has a 2D-layered anionic framework in the ab plane (Fig. 2a), while each $[\text{SiO}_4]$ tetrahedron shares three O corners with neighboring $[\text{MgO}_6]$ octahedrons to form a corrugated layer along the c -axis (Fig. 2b). The Ca(1) ions are embedded in the corrugated layer framework, whereas the Ca(2) ions occupy the sites between the layers (Fig. 2b).

Previously, Moore studied the structure of merwinite [6], which had the space group $P2_1/c$. It is very common for the silicates to transform from a P-lattice to a C-lattice as temperature increases. The sort of phase transition could also be induced by high pressure [23–27]. In clinopyroxenes, for example, there are two different and symmetrically-independent tetrahedron chains, which become indistinguishable at the transition temperature [23]. In the merwinite structure, the 2D layer is linked by two different and independent [Si-O-Mg] chains along the ab -plane, whereas in the new $\text{Ca}_3\text{MgSi}_2\text{O}_8$ compound the two

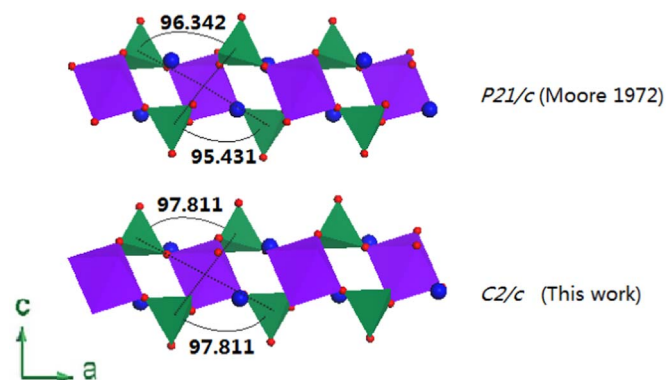


Fig. 3. Chain of $[\text{SiO}_4]$ tetrahedra linked with $[\text{MgO}_6]$ octahedra.

[Si-O-Mg] chains are identical (Fig. 3).

3.3. Isothermal bulk modulus

The enthalpies of the new $\text{Ca}_3\text{MgSi}_2\text{O}_8$ compound and the merwinite have been calculated at 0 K and 0 GPa. They are negative, with the enthalpy of the new structure being 0.006 meV/atom higher than that of the merwinite. The geometry parameters of the new $\text{Ca}_3\text{MgSi}_2\text{O}_8$ compound at zero pressure obtained from the first-principles simulation are summarized in Table S3. As usual, the unit-cell parameters and bond lengths calculated by the GGA method are slightly larger (0.06–3.44%) than our experimental determinations, indicating that our theoretical simulation well reproduces the crystallographic data of the new $\text{Ca}_3\text{MgSi}_2\text{O}_8$ compound (e.g., [5,28,29]).

The unit-cell parameters of the new $\text{Ca}_3\text{MgSi}_2\text{O}_8$ compound at different pressures are shown in Fig. 4. All unit-cell parameters vary non-linearly with P for the investigated P range. To determine the isothermal bulk modulus, the third-order Birch-Murnaghan equation of state (BM-EoS) [30] has been fitted with the P - V data by a least-squares method:

$$P(V) = \frac{3B_0}{2} \left[\left(\frac{V_0}{V} \right)^{\frac{7}{3}} - \left(\frac{V_0}{V} \right)^{\frac{5}{3}} \right] \times \left\{ 1 + \frac{3}{4} (B'_0 - 4) \left[\left(\frac{V_0}{V} \right)^{\frac{2}{3}} - 1 \right] \right\}, \quad (1)$$

where P is the pressure, B_0 the isothermal bulk modulus, B'_0 the first pressure derivative of B_0 , V_0 the volume at zero pressure and V the volume at high pressures. When B'_0 is set as 4, the B_0 of the $\text{Ca}_3\text{MgSi}_2\text{O}_8$ compound is 97.1(5) GPa and the V_0 is 681.6(1) Å³. If B'_0 is not fixed, the results of our best data-fitting are $B_0 = 99(2)$ GPa, $B'_0 = 3.5(5)$, and $V_0 = 681.5(2)$ Å³. A linearized third-order Birch-Murnaghan equation of state [31] was used to obtain the parameters of the equations of state for the crystallographic axes, yielding: $a_0 = 9.580(6)$ Å, $B_{0-a} = 60(2)$

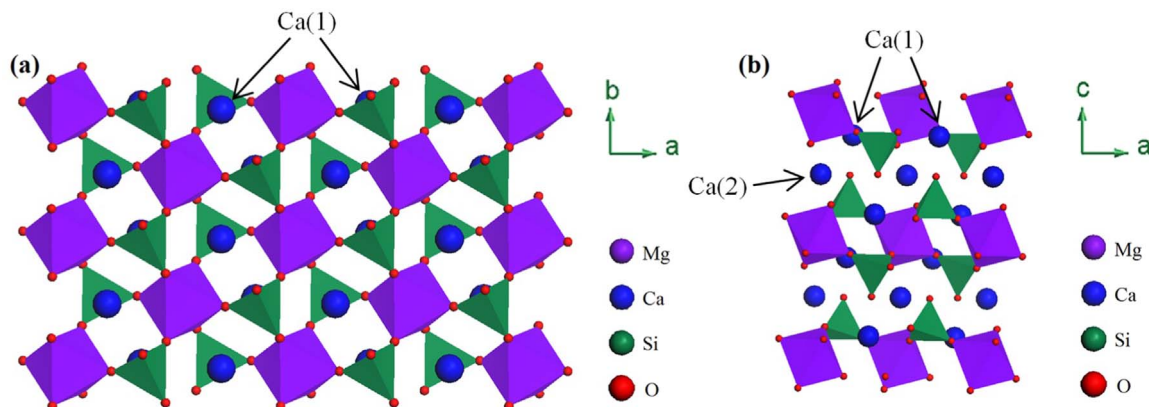


Fig. 2. Polyhedral view on the structure of the new $\text{Ca}_3\text{MgSi}_2\text{O}_8$ compound along the [001] direction (a) and [010] direction (b).

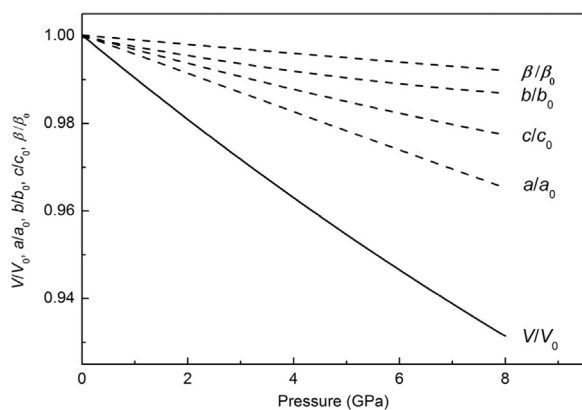


Fig. 4. Pressure dependence of normalized unit-cell parameters (a/a_0 , b/b_0 , c/c_0 , β/β_0 , V/V_0) of the new $\text{Ca}_3\text{MgSi}_2\text{O}_8$ compound at 0 K.

GPa for the a -axis, $b_0 = 5.308(2)$ Å, $B_{0-b} = 183(8)$ GPa for the b -axis, and $c_0 = 13.420(2)$ Å, $B_{0-c} = 100(1)$ GPa for the c -axis, if the B'_{0-a} , B'_{0-b} , and B'_{0-c} are fixed as 4.

3.4. Heat capacity and entropy

We calculated the phonon dispersions and VDoS of the new $\text{Ca}_3\text{MgSi}_2\text{O}_8$ compound by the first-principles method using density functional perturbation theory. The dynamical matrices were computed at 24 wave (q) vectors in the Brillouin zone of the primitive cell, and interpolated to obtain the bulk phonon dispersions. Fig. 5 shows the predicted dispersion curves along several symmetry directions and the VDoS. The result suggests that the new $\text{Ca}_3\text{MgSi}_2\text{O}_8$ compound is dynamically stable. On the other hand, our preliminary simulation work using the merwinite structural data from Moore et al. [6] always led to some imaginary phonon frequencies in the phonon dispersions, indicating a dynamical instability [32].

The results of the phonon spectra for the $\text{Ca}_3\text{MgSi}_2\text{O}_8$ compound were used to compute the internal energy (E) and isochoric heat capacity (C_v) as functions of temperature as well. The temperature dependence of the E was obtained by the following equation,

$$E(T) = E_{tot} + E_{zp} + \int \frac{h\omega}{\exp\left(\frac{h\omega}{kT}\right) - 1} F(\omega) d\omega, \quad (2)$$

with E_{tot} representing the total electronic energy at 0 K, E_{zp} the zero point vibrational energy, h the Planck's constant, k the Boltzmann constant, and $F(\omega)$ the vibrational density of states. We evaluated the E_{zp} in Eq. (2) using the following equation,

$$E_{zp} = \int F(\omega) h\omega d\omega. \quad (3)$$

Furthermore, we approximated the lattice contribution to the C_v with the following equation:

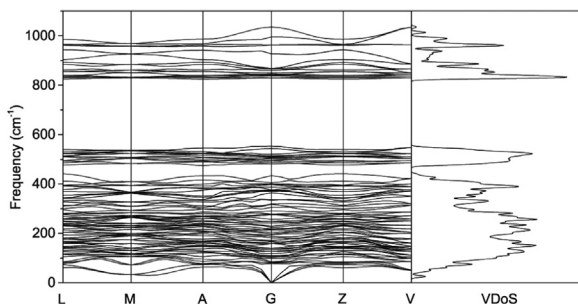


Fig. 5. Phonon dispersions and VDoS of the new $\text{Ca}_3\text{MgSi}_2\text{O}_8$ compound.

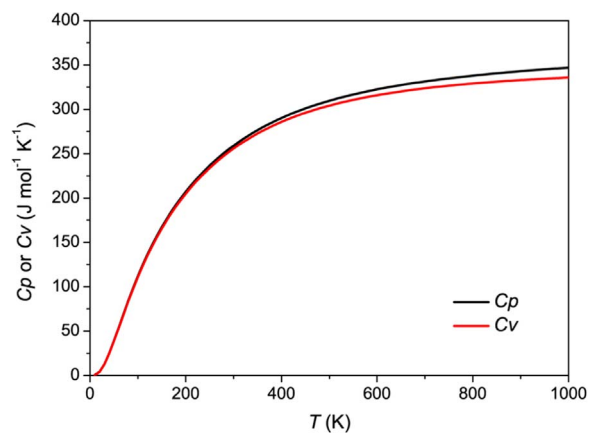


Fig. 6. Isochoric and isobaric heat capacity (C_p and C_v , respectively) of the new $\text{Ca}_3\text{MgSi}_2\text{O}_8$ compound.

$$C_v(T) = k \int \frac{\left(\frac{h\omega}{kT}\right)^2 \exp\left(\frac{h\omega}{kT}\right)}{\left[\left(\frac{h\omega}{kT}\right)^2 - 1\right]^2} F(\omega) d\omega. \quad (4)$$

The C_v result calculated in this way is shown in Table S4.

The C_p was calculated by adding an anharmonic effect to the C_v obtained from the above calculations, using the following equation:

$$C_p = C_v + \alpha_T^2 B_T V_T T, \quad (5)$$

where α_T , B_T , and V_T are the thermal expansion coefficient, isothermal bulk modulus, and volume at 1 atm and T (K), respectively. We assumed the α_T of the new $\text{Ca}_3\text{MgSi}_2\text{O}_8$ compound as $3.33 \times 10^{-5} \text{ K}^{-1}$ by averaging the values of the β - Ca_2SiO_4 ($4.24 \times 10^{-5} \text{ K}^{-1}$) [5] and the CaMgSiO_4 ($2.42 \times 10^{-5} \text{ K}^{-1}$) [33]. The temperature derivative of B_T has not been experimentally determined as well, and assumed as zero in our calculation. V_T at T K was calculated with the following equation:

$$V_T = V_{298} \exp\left(\int_{298}^T \alpha_T dT\right), \quad (6)$$

where $V_{298} = 99.2(2) \text{ cm}^3/\text{mol}$. The calculated C_p values are listed in Table S4 and shown in Fig. 6. Errors of our C_p values were propagated from the uncertainty in the volume and isothermal bulk modulus, and they decrease from $\sim 0.38\%$ at ~ 10 K to $\sim 0.02\%$ at ~ 120 K, and then increase to $\sim 0.07\%$ at 1000 K. The calculated C_p data were then expressed using the following polynomial of temperature,

$$C_p = k_0 + k_1 T^{-0.5} + k_2 T^{-2} + k_3 T^{-3} + k_4 T + k_5 T^2 + k_6 T^3, \quad (7)$$

where C_p is in $\text{J mol}^{-1} \text{ K}^{-1}$ and T in K. In the fitting procedure, the data were divided into three different T intervals, 10–80 K, 80–298 K, 298–1000 K. The C_p equation coefficients for the three T intervals are summarized in Table S5.

The obtained C_p values have been applied to the calculation of the vibrational entropy at T K using the following equation,

$$S_T^0 = \int_0^T \frac{C_p}{T} dT. \quad (8)$$

The vibrational entropy at 298 K (S_{298}^0) calculated from the C_p values in the T range of 0–298 K obtained in this study is $270.5(60) \text{ J mol}^{-1} \text{ K}^{-1}$.

4. Conclusion

Mineral inclusions with the composition $\text{Ca}_3\text{MgSi}_2\text{O}_8$ were discovered in some diamonds [34], and conventionally treated as merwinite

with the $P21/a$ space group. Our result suggests that the $\text{Ca}_3\text{MgSi}_2\text{O}_8$ mineral inclusions at the P-T conditions of the mantle might have the $C2/c$ space group. With some investigations on the crystal structure and thermodynamic properties of this new $\text{Ca}_3\text{MgSi}_2\text{O}_8$ compound, we have reached the following conclusions:

1. This new $\text{Ca}_3\text{MgSi}_2\text{O}_8$ compound crystallizes in the $C2/c$ space group with $a = 9.344(4) \text{ \AA}$, $b = 5.308(3) \text{ \AA}$, $c = 13.290(6) \text{ \AA}$, $\alpha = 90^\circ$, $\beta = 92.072(7)^\circ$, $\gamma = 90^\circ$, and $V = 658.7(6) \text{ \AA}^3$. The theoretical simulation of compressional behaviors and phonon dispersion suggest that the new compound is thermally and dynamically stable;
2. The isothermal bulk modulus B_0 of this new $\text{Ca}_3\text{MgSi}_2\text{O}_8$ compound has been theoretically obtained as 99(2) GPa, with its first pressure derivative B'_0 as 3.5(5);
3. The isobaric heat capacity C_p and standard vibrational entropy S_{298}^0 of this new $\text{Ca}_3\text{MgSi}_2\text{O}_8$ compound have been theoretically determined as $C_p = 3.927(2) \times 10^2 - 1.159(6) \times 10^3 T^{-0.5} - 1.054(4) \times 10^7 T^{-2} + 1.362(8) \times 10^9 T^{-3} \text{ J mol}^{-1} \text{ K}^{-1}$ for the T range of 298–1000 K and $S_{298}^0 = 270.5(60) \text{ J mol}^{-1} \text{ K}^{-1}$.

Acknowledgements

This study was financially supported by the Strategic Priority Research Program (B) of Chinese Academy of Sciences (Grant No. XDB18000000), by the DREAM project of MOST, China (Grant No. 2016YFC0600408), and by the Program of the Data Integration and Standardization in the Geological Science and Technology from MOST, China (Grant No. 2013FY1109000-3).

Appendix A. Supporting information

Supplementary data associated with this article can be found in the online version at [doi:10.1016/j.jssc.2017.08.005](https://doi.org/10.1016/j.jssc.2017.08.005).

References

- [1] J. Kim, P. Jeon, J. Choi, H. Park, S. Mho, G. Kim, *Appl. Phys. Lett.* 84 (2004) 2931–2933.
- [2] C. Wu, J. Chang, J. Wang, S. Ni, W. Zhai, *Biomaterials* 26 (2005) 2925–2931.
- [3] M. Maćzka, J. Hanzab, A. Kaminski, S. Kojima, *J. Alloy. Comp.* 638 (2015) 34–37.
- [4] W. Joswig, T. Stachel, J. Harris, W. Baur, G. Brey, *Earth Planet. Sci. Lett.* 173 (1999) 1–6.
- [5] Z. Xiong, X. Liu, S.R. Shieh, S. Wang, L. Chang, J. Tang, X. Hong, Z. Zhang, H. Wang, *Am. Miner.* 101 (2016) 277–288.
- [6] P.B. Moore, T. Araki, *Am. Miner.* 57 (1972) 1355–1374.
- [7] L. Liu, *Contrib. Mineral. Petrol.* 69 (2002) 245–247.
- [8] M. Kanzaki, X. Xue, Y. Wu, S. Nie, *Phys. Chem. Miner.* <http://dx.doi.org/10.1007/s00269-017-0896-z>.
- [9] Q. He, X. Liu, B. Li, L. Deng, Z. Chen, X. Liu, H. Wang, *Phys. Chem. Miner.* 40 (2013) 29–40.
- [10] L. Chang, X. Liu, C. Wu, X. Liu, G. Li, *Phys. Chem. Miner.* 42 (2015) 223–234.
- [11] X. Liu, M. Fleet, *J. Mineral. Petrol. Sci.* 104 (2009) 25–36.
- [12] Bruker, SAINT+, Version 6.02, Bruker AXS Inc, Madison, Wisconsin, USA, 1999.
- [13] G. Sheldrick, SADABS, Version 2.03, University of Göttingen, Germany, 1996.
- [14] G. Sheldrick, A Program for Automatic Solution of Crystal Structure, University of Göttingen, Germany, 1997.
- [15] G. Sheldrick, A Program for Crystal Structure Refinement, University of Göttingen, Germany, 1997.
- [16] P. Hohenberg, W. Kohn, *Phys. Rev.* 136 (1964) 864–871.
- [17] W. Kohn, L. Sham, *Phys. Rev.* 140 (1965) 1133–1138.
- [18] M. Payne, M. Teter, D. Allan, T. Arias, J. Joannopoulos, *Rev. Mod. Phys.* 64 (1992) 1045–1097.
- [19] J. Perdew, K. Burke, M. Ernzerhof, *Phys. Rev. Lett.* 77 (1996) 3865–3868.
- [20] J. Lin, A. Qteish, M. Payne, V. Heine, *Phys. Rev. B* 47 (1993) 4147–4180.
- [21] M. Lee, Advanced Pseudopotentials For Large Scale Electronic Structure Calculations (Ph.D. thesis), University of Cambridge, 1995.
- [22] H. Monkhorst, J. Pack, *Phys. Rev. B* 13 (1976) 5188–5192.
- [23] T. Arlt, T. Armbruster, *Eur. J. Mineral.* 9 (1997) 953–964.
- [24] T. Arlt, R.J. Angel, R. Miletich, T. Armbruster, T. Peters, *Am. Mineral.* 83 (1998) 1176–1181.
- [25] T. Arlt, M. Kunz, J. Stolz, T. Armbruster, R.J. Angel, *Contrib. Mineral. Petrol.* 138 (2000) 35–45.
- [26] M. Tribaudino, F. Nestola, F. Camara, M. Domeneghetti, *Am. Mineral.* 87 (2002) 648–657.
- [27] M. Tribaudino, F. Nestola, C. Meneghini, G.G. Bromiley, *Phys. Chem. Miner.* 30 (2003) 527–535.
- [28] Y. Zhang, X. Liu, Z. Xiong, Z. Zhang, *Sci. China Ser. D* 59 (2016) 989–996.
- [29] Y. Zhang, X. Liu, S.R. Shieh, X. Bao, T. Xie, F. Wang, Z. Zhang, C. Prescher, V.B. Prakapenka, *Phys. Chem. Miner.* 44 (2016) 1–15.
- [30] F. Birch, *Phys. Rev.* 71 (1947) 809–824.
- [31] R. Angel, EosFit, Version 5.2, Virginia Tech, Blacksburg, Virginia, USA, 2000.
- [32] Z. Xiong, High temperature and high pressure study about the Ca-rich silicates in the system $\text{Ca}_2\text{SiO}_4\text{-Ca}_3\text{MgSi}_2\text{O}_8$ (Ph.D. thesis), Peking University, 2015.
- [33] R. Lager, E. Carmichael, *Am. Mineral.* 63 (1978) 365–377.
- [34] D.A. Zedgenizov, A. Shatskiy, A.L. Ragozin, H. Kagi, V. Shatskiy, *Am. Mineral.* 99 (2014) 547–550.